

Asymmetric oscillations during phase separation under continuous cooling - A simple model

Yumino Hayase^a), Mika Kobayashi, Doris Vollmer, Harald Pleiner, and
Günter K. Auernhammer

Max Planck Institute for Polymer Research, 55128 Mainz, Germany

(Received 3 September 2008; accepted 8 October 2008; published online 2008)

We investigate the phase separation of binary mixtures under continuous cooling using the Cahn - Hilliard equation including the effect of gravity. In our simple model, sedimentation is accounted for by instantaneously "removing" droplets from the supersaturated mixture into the coexisting phase once the droplets have reached a defined maximum size. Our model predicts an oscillatory variation of turbidity. Depending on the composition either both phases oscillate (symmetric oscillations) or only one of the phases oscillates (asymmetric oscillations). In the asymmetric case, droplet sedimentation from the majority phase into the minority phase reduces supersaturation in the minority phase. This inhibits droplet formation in the minority phase. The cooling rate dependence of the period agrees with experimental results. © 2008 American Institute of Physics.

[DOI: 10.1063/1.3009867]

I. INTRODUCTION

The dynamics of phase separation strongly depends on the thermal protocol, for example whether phase separation is induced by a temperature quench from a one-phase to a two-phase system,^{1,2} by a double temperature quench, or by slow continuous ramping. In the latter case, qualitatively new features can arise, like oscillations of the turbidity and apparent heat capacity.³⁻⁸

Oscillatory phase separation in volume-dominated systems has been observed in several systems as different as microemulsions,³ polymer solutions⁴ and even mixtures of olive oil and methanol.⁵ It is a universal phenomenon that can be found, both in low molecular weight and polymer mixtures. Its qualitative behavior does not depend on whether the mixture phase separates under heating³ or cooling.^{4,5}

Oscillatory phase separation proceeds as follows:^{4,6} For simplicity, we adopt the notation of systems which are phase separating under cooling. A binary mixture is prepared in the one-phase and cooled into the two-phase region (Fig.1a). After crossing the binodal curve (cloud point) supersaturation of the homogeneous mixture induces nucleation, which is followed by droplet growth and coarsening. When the droplets have reached a size of a few hundreds of nm, the mixture appears turbid due to the scattering of light in the generally not index matched mixtures. Upon further growth and coarsening of the droplets, gravity causes their sedimentation. After sedimentation, the system is transparent again. However, the two coexisting phases are separated by an interface. Continuous cooling of the phase separated system, again leads to supersaturation in both coexisting phases. Depending on the supersaturation in each phase droplets nucleate in both phases or only in one. Again, the newly created droplets grow, coarsen and sediment. This cycle (Fig.1b) may repeat itself several times (in some expe-

periments up to 20 times) until the coexisting phases are sufficiently poor in their respective minority component such that the latter can be molecularly dissolved at all temperatures. Theoretical studies were started by J. Vollmer et al.^{5,6,9} They pointed out that the oscillations arise due to an interplay of processes connected to well-separated time scales, i.e. slow increase of supersaturation vs. fast relaxation (reduction of supersaturation). They predict that the oscillations arise from thermodynamics and are not of hydrodynamic origin. Although sedimentation of droplets and surface tension cause convection in both phases, convection is assumed to homogenize the temperature, but does not determine the period of the oscillations. Vollmer et. al. observed an oscillatory phase separation and even a limit cycle for a well defined parameter range.^{5,9} However, their model did not consider spatial degrees of freedom.

Hydrodynamic effects are explicitly considered in a theoretical approach based on the Navier-Stokes equation, which is coupled to the nonlinear advection-diffusion equation.^{10,11} These studies were motivated by a weak container size dependence of the period of the oscillations in thin cells.¹² A size dependence is characteristic for most hydrodynamic instabilities, for example for the Rayleigh-Bénard instability. In analogy to the latter instability, the oscillations were expected to be due to the density difference between the top and bottom of the container and the density close to the interface. Indeed, Lattice Boltzmann simulations showed an oscillatory instability. However, the numerical results differed by several orders of magnitude from the experimental parameter range.^{10,11}

No previous theoretical studies discussed the difference of the dynamics between the upper and the lower phase, i.e. asymmetric oscillations. Experimentally, it was observed that often only the turbidity of the upper phase oscillates and the average turbidity of the lower phase remains almost constant (see in Fig.1b,c). Our aim is to explain this asymmetry using a simple model.

We use the Cahn - Hilliard (CH) equation^{13,14} for phase sep-

^a)Electronic mail: hayase@mpip-mainz.mpg.de

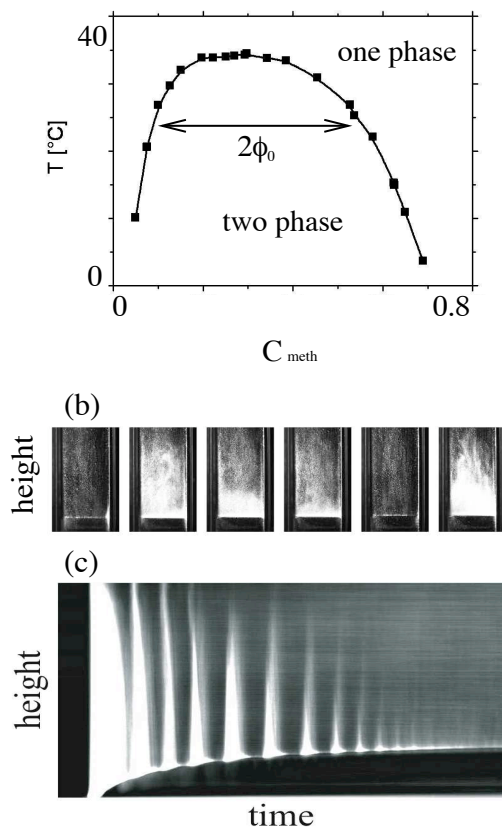


FIG. 1: (a) Part of the phase diagram for mixtures of methanol - hexane. The points depict the experimentally determined phase-transition temperatures, as determined from turbidity measurements. $2\phi_0$ denotes the width of the biphasic region.

(b) Snapshots of the observed oscillatory phase separation under continuous cooling at a rate of 10 K/h. Volume fraction of methanol $C_{meth} = 0.2$. Images were taken after 1010 s (33.2 °C), 1085 s (33.0 °C), 1135 s (32.8 °C), 1150 s (32.8 °C), 1260 s (32.5 °C), 1385 s (32.2 °C), from left to right, respectively. The white part indicates that droplets exist and dark part indicates that the system is transparent. The system suddenly becomes turbid, and after a while, it becomes transparent again due to droplet sedimentation. These processes are repeating.

(c) Space-time plot of turbidity oscillations at 10 K/h from 36 °C to 26 °C. It is obtained by assembling line data, which were integrated snapshots in horizontal direction. The total time is 3600 s.

ation under continuous cooling, and include gravity-induced volume exchange as the coupling parameter between the upper and the lower phase. The CH equation is derived from a Ginzburg-Landau free energy functional.^{13,14} It is a partial differential equation describing a system with a conserved order parameter. Phase-ordering dynamics after a temperature jump from the one-phase region to the two-phase region has been studied analytically and numerically using the CH equation.¹⁵⁻¹⁷ In the case of continuous cooling, studies using the CH equation did not yield an oscillatory instability.¹⁸ Various possibilities on how to include gravity in the CH equation are discussed in Refs.¹⁹⁻²¹. Kitahara et al.¹⁹ pointed out

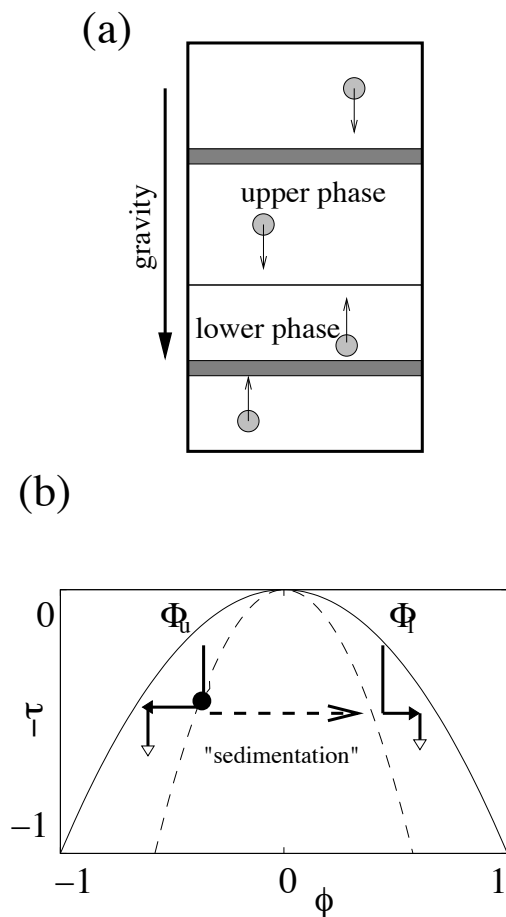


FIG. 2: (a) The model system consists of two phases, in the upper and lower space, each of which is assumed to be homogeneous in the gravity direction. Each phase is described within a horizontal region (gray region).

(b) Scheme of the temperature - composition behavior. The thick lines indicate the composition of the upper/lower phase $\Phi_{u/l}$. At the black circle, droplets are created in the upper phase, which grow and sediment later by moving to the lower phase. The dashed arrow indicates the shift of composition due to droplets exchange.

that the mobility should depend on the order parameter, when a gravity term is added to the free energy. More quantitative studies were able to predict droplet sedimentation during phase separation^{22,23}. According to our knowledge, the combination of gravity and continuous cooling has not yet been investigated using the CH model.

In the sedimentation of droplets, of course, hydrodynamics affects coarsening. The phase separation dynamics including hydrodynamical effects has been studied by using "model H"²⁴⁻²⁶ in the Hohenberg-Halperin notation.²⁷

Since experimental findings point towards a thermodynamic origin of the oscillations, we only include strongly simplified hydrodynamic contributions. In this paper, we investigate the CH equation for continuous cooling including a model for gravity, focussing on the interplay between the up-

per and the lower phase. We find that the composition before the phase separation (total composition, Φ_{tot}) decides which phase oscillates. We also discuss the dependence of the oscillation frequency on the cooling rate.

II. EXPERIMENTAL

A. Sample Preparation

Methanol and hexane (both analytic grade) were purchased from Sigma-Aldrich and used as supplied. The samples were prepared by mixing the appropriate amounts of the respective components. The mixtures were loaded into teflon-sealed fluorescence cuvettes (width \times depth \times height: $1 \times 1 \times 4 \text{ cm}^3$). The mixture was continuously stirred and kept at a temperature well within the single-phase region before starting the experiments.

B. Optical set-up

The homogenized sample was placed in a transparent water bath (resembling a fish tank). The water temperature was controlled by a Haake thermostat to an accuracy of better than 0.1 K . Detailed temperature protocols can be followed automatically and the temperature setting is recorded together with the optical data.⁴ The intensity of the scattered light was measured by video microscopy. The two-dimensional intensity distribution of individual snap shots (Fig.1b) are averaged horizontally. The resulting vertical turbidity profiles of successive images are set together to the space-time plots shown in Fig.1c. Dark areas in the space-time plot correspond to periods in which the sample was transparent and bright areas correspond to turbid periods (see Fig.1c).

III. MODEL

A. Phase separation

The CH equation^{13,14} describes the temporal evolution of the "order parameter" $\phi(r, t)$, which denotes the deviation of the composition from its average value, as a function of space, r and time t .

$$\frac{\partial \phi}{\partial t} = \nabla^2(-\epsilon^2 \nabla^2 \phi + \phi[\tau(t) - \phi^2]). \quad (1)$$

The total composition Φ_{tot} is calculated from the order parameter $\phi(r, t)$ by $\Phi_{tot} = \frac{1}{V} \int_V d^3r \phi(r, t)$. Here, V is the volume of the system. The CH equation is derived from the ϕ^4 free-energy functional. The parameter ϵ denotes the ratio between the interfacial width and the size of a nuclei of a mesoscopically phase separated domain. The phenomenological dimensionless parameter τ measures the temperature difference to the critical temperature T_c . τ is negative if the mixture is one-phase, i.e. $T > T_c$. For the CH equation one

usually takes a positive value of τ to study phase separation processes after a temperature jump into the two phase region $T < T_c$. For a continuously ramped temperature, τ is positive and an increasing function of time.

The average mass transfer between the coexisting phases depends on the width of the coexistence region $2\phi_0$ as shown in Fig.1a. To keep the average mass transfer constant, we have adjusted the cooling rate to the slope of the phase diagram. This implies that the reduced cooling rate ξ has to be held constant:⁴

$$\xi[\tau(t)] = \frac{1}{\phi_0[\tau(t)]} \frac{\partial \phi_0[\tau(t)]}{\partial t}. \quad (2)$$

Experimentally, it has been observed that the number of oscillations strongly increases, when keeping the mass transfer constant.⁴ For the CH equation, the width of the coexistence region is equal to the square root of τ ,

$$\phi_0 = \pm \sqrt{\tau} \quad (3)$$

Keeping ξ constant leads to an exponential increase of τ with time.

$$\tau(t) = \tau_0 \exp(2\xi t). \quad (4)$$

$\tau(t)$ changes from $\tau = \tau_0$ to $\tau = \tau_{end}$.

The experimental system is prepared in the one-phase region and rapidly cooled to a temperature just under the binodal line in order to create an interface between the upper and lower phase. After the system has equilibrated, it is slowly cooled into the two-phase region (Eq.(2)). In the simulation, the initial temperature τ_0 is a value in the two-phase region close to the binodal line, Eq.(3). The initial temperature must be chosen below the binodal, i.e. $\tau_0 < \Phi_{tot}^2$. For simplicity $\tau_{end} = 1$ is used.

The CH equation, modified by a term accounting for continuous cooling does not give rise to an oscillatory instability.¹⁸ This can be understood from the following scaling argument: The time scale of radius coarsening²⁸ is $< R > \sim t^{1/3}$, while the mean square displacement of diffusion is proportional to t . Since the coarsening is slower than diffusion, the order parameter in the domains cannot reach supersaturation after the domains are formed. Gravity effectively increases the growth rate of interdroplet distances by sedimentation.

B. Gravity

The CH equation can be modified by adding a potential resembling the gravitational field¹⁹⁻²¹. Using this modified CH equation, phase separation by a temperature jump has been investigated numerically.^{22,23} Since these studies focused on sedimentation, they did not imply a zero flux boundary condition. The latter, however, is important in the present system, since ϕ is conserved and the system under investigation is finite and closed. Therefore one must enforce zero flux in the direction of gravity as a boundary condition. This considerably complicates the numerical solution of the CH equation, and therefore we do not take this approach. Instead we add a

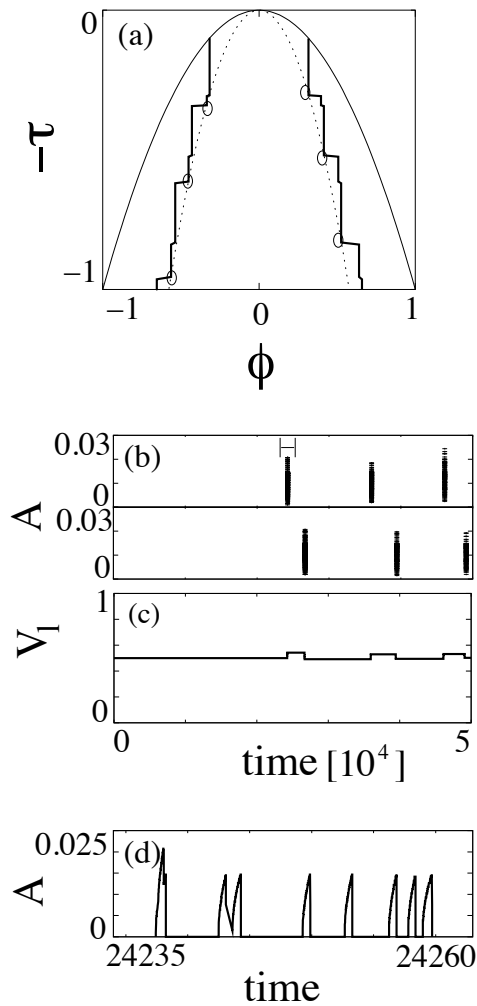


FIG. 3: Symmetric oscillations: (a) Evolution of the compositions $\Phi_{u/l}$. At the open circles, the upper/lower phase nucleates droplets. (b) Time evolution of the total droplet area. The upper and lower parts of the figure correspond to the turbidity of the upper and lower phase, respectively. (c) Time evolution of the volume of the lower phase. (d) Enlarged display of the first nucleation sequence shown in (b) of the upper phase at $t \approx 2.4 \times 10^4$. The total composition $\Phi_{tot} = 0$, the initial temperature $\tau_0 = 0.1$, the reduced cooling rate $\xi = 2.3 \times 10^{-5}$, the system size $L = 32$, the critical domain radius $R_c = 15/128 \approx 0.117$, and the parameter in the CH equation $\epsilon = 0.01$.

simple rule to the CH equation, Eq.(1), mimicking sedimentation in a gravity field as explained now.

We divide the sample into two systems representing the upper and lower phases. Both systems independently obey the CH equation modified to account for slow cooling. The coupling between the systems is accounted for by the following rule: when a droplet has reached its critical radius R_c , it is taken out of one phase and added to the other. This resembles instantaneous sedimentation of droplets.

This ansatz is motivated by the experimental fact that droplets are most efficient in collecting supersaturation when

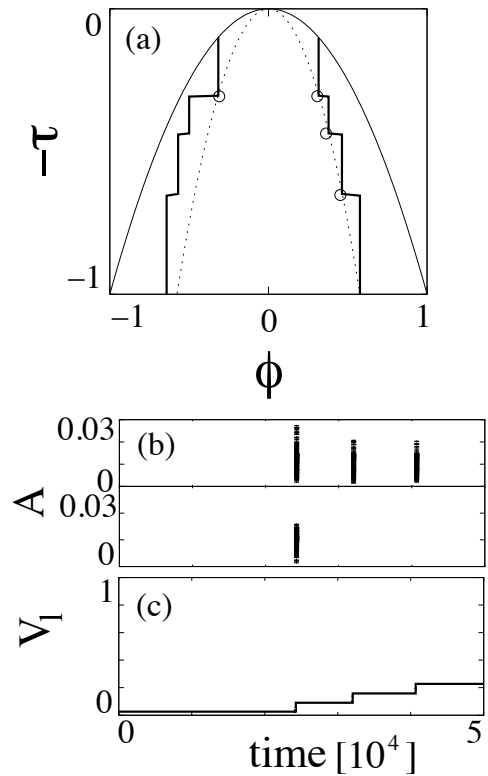


FIG. 4: Asymmetric oscillations: (a) Evolution of the compositions $\Phi_{u/l}$. (b) Time evolution of the total droplet area, which is a measure for the turbidity. (c) Time evolution of the volume of the lower phase. The total composition $\Phi_{tot} = 0.3$, while the other parameters are identical to those in Fig. 3.

they are small and have a high number density and a large surface to volume ratio. As they grow, they merge, their number density strongly decreases, and droplets start to sediment. As a result of these processes, their efficiency to collect supersaturation strongly decreases. The critical droplet size can be estimated equating thermal and gravitational energy. The particles settle, if gravitational energy $F_G = 4/3\pi R^3 \Delta\rho g h$ dominates over thermal energy, $F_B = k_B T$, where R denotes the radius of the droplet, g the earth's gravity constant, and $\Delta\rho$ the density difference between the droplet and the surrounding matrix. To estimate this size, we take the height difference h to be typically of the order of a particle diameter. Balancing both energies yields R_c , the 'critical' radius with $R_c^4 = 3k_B T / (4\pi \Delta\rho g)$. For mixtures of methanol and hexane ($\Delta\rho \approx 0.1 \text{ gcm}^{-3}$) this gives $R_c = 1 \mu\text{m}$.

For simplification, we assume homogeneity in the vertical direction, choose one horizontal region for each phase (Fig.2a) and solve the CH equation only on the two regions. To take into account the volume of both phases, we introduce the volume of the upper/lower phase, $V_{u/l}$, and the composition of the upper/lower phase, $\Phi_{u/l}$. The value of $\Phi_{u/l}$ is calculated from the order parameter $\phi_{u/l}(r, t)$ in the upper/lower

phase by $\Phi_{u/l} = V_{u/l}^{-1} \int_{V_{u/l}} d^3r \phi_{u/l}(r, t)$. This setting avoids the difficulty of the zero flux boundary condition in the direction of gravity.

When a droplet in the upper phase with volume V_d and composition Φ_d moves into the lower phase, the volume of the upper/lower phase and the composition change to the new values $V'_{u/v}$ and $\Phi'_{u/v}$. The system has to fulfill two conservation laws, i.e. volume conservation $V_l + V_u = V'_l + V'_u = V$ ($\equiv 1$) and composition conservation $\Phi_l V_l + \Phi_u V_u = \Phi'_l V'_l + \Phi'_u V'_u = \Phi_{tot}$. Moving a droplet from the upper phase to the lower yields two additional equations

$$V'_l = V_l + V_d \quad (5)$$

$$\Phi'_l = \frac{\Phi_l V_l + \Phi_d V_d}{V_l + V_d}. \quad (6)$$

When a droplet in the lower phase moves into the upper phase, the index l in the equations (5) and (6) are replaced by the index u .

Fig.2b sketches a typical evolution of the compositions due to droplet exchange, i.e. due to instantaneous sedimentation. Under cooling, the compositions of the upper and the lower phases remain constant (the evolution is indicated by the vertical lines.). Supersaturation must be sufficiently high to make nucleation favorable. As we only allow for homogeneous nucleation, droplets nucleate only near the spinodal. They rapidly grow diffusively thereby reducing supersaturation. As soon as they have reached the 'critical' size at the temperature marked by the black circle in Fig.2b, the composition of the upper phase moves toward the binodal line. Importantly, as the droplets are added to the lower phase also the composition of the lower phase moves towards the binodal line, i.e. supersaturation is reduced in both phases.

Summing up, we have introduced "gravity" ignoring hydrodynamics, i.e. solvent flow. Our model should describe oscillatory phase separation well, if the built-up of supersaturation is slow compared to its relaxation. Our model fulfills all conservation laws and is very simple to implement numerically.

C. Numerical conditions

To test our ansatz we investigated the dependence of the resulting composition oscillations on the initial total composition and the cooling rate. The numerical simulations were carried out for $\epsilon = 0.01$ and 0.02 . We take the region as a 1-dimensional system. We chose three system sizes $L = 16, L = 32$, and $L = 64$, corresponding to 2048, 4096, and 8192 points, respectively for a spatial mesh $dr = 1/128 \sim 0.0078$. We chose a time step $dt = 0.01$ and used periodic boundary conditions for each slice. We solved the CH equation using the Fast Fourier transformation method.²⁹ All results presented have been checked to be qualitatively insensitive to changes in dr and dt . We took the critical domain radii $R_c = 15dr \sim 0.117$ and $25dr \sim 0.195$ corresponding to 15 and 25 points, respectively.

The system has three length scales, the system size L , the critical domain radius R_c and the domain width ϵ . In the numerical simulation, the critical radius R_c is about 10 times larger than ϵ , and the system size L is 100 times larger than the critical radius R_c , i.e. the three length scales are well separated. The oscillation properties described in the following are not sensitive to a change of the critical radius by at least a factor of 2.

There are three relevant parameters, i.e. the total composition Φ_{tot} , the initial temperature τ_0 and the cooling rate ξ . Φ_{tot} and τ_0 define the initial condition. The simulations start after the formation of an interface between upper and lower phases. We assume that both phases have reached equilibrium at $t = 0$. This is equivalent to the experiments, in which the slow cooling starts after all processes due to the initial phase separation have relaxed, and an interface between the two phases has formed. The initial composition of the upper/lower phase, $\Phi_{u/l}(t = 0)$ is taken as its value on the binodal line at τ_0 , and we take Φ_l to be positive and Φ_u negative. The volume of the upper/lower phase $V_{u/l}(t = 0)$ is calculated considering volume and composition conservation as explained before. Each phase has an order parameter $\phi_{u/l}(r, t)$, which describes the spatial variation of the composition in that phase. Initially, $\phi_{u/l}(r, t = 0)$ is uniformly distributed beside of random fluctuations around $\Phi_{u/l}(t = 0)$.

We add conserved noise to the order parameter $\phi(r, t)$. The conserved noise²⁹ has the property $\langle \zeta(r, t) \rangle = 0$ and $\zeta(r, t) = \zeta_0(r, t) - 0.5[\zeta_0(r - dr, t) + \zeta_0(r + dr, t)]$, with $\zeta_0(r, t)\zeta_0(r + dr, t + dt) = \zeta_0^2 \delta(dr)\delta(dt)$. The scenario described below is rather robust against changes in the noise strength. We also investigated the non-conserved noise, i.e. $\langle \zeta(r, t) \rangle = 0$ and $\zeta(r, t)\zeta(r + dr, t + dt) = \zeta_1^2 \delta(dr)\delta(dt)$. However, the scenario described is robust against changes in the nature of the noise. When the noise strength increases, the period of the oscillation decreases.

IV. RESULTS

A. Composition dependence

Figure 3 shows the numerical results of our model at a total composition $\Phi_{tot} = 0$, an initial temperature $\tau_0 = 0.1$, and a reduced cooling rate $\xi = 2.3 \times 10^{-5}$. At $\Phi_{tot} = 0$, the volume of the upper and the lower phases are equal, $V_l(t = 0) = V_u(t = 0) = 0.5$. According to Eq.(3), $\tau_0 = 0.1$ implies for the initial composition $\Phi_u(t = 0) = -\Phi_l(t = 0) = \sqrt{\tau_0} \approx 0.32$.

Figure 3a depicts the evolution of $\Phi_{l/u}$. The right/left thick line indicates the temporal evolution of the compositions of the upper/lower phase. As $\Phi_u(t = 0) = -\Phi_l(t = 0)$, in the beginning the supersaturation in both phases increases identically. Nucleation of droplets is as probable in the upper as in the lower phase and therefore determined by noise. In this simulation, the upper phase happens to first nucleate droplets at about $\tau = 0.3$. Figure 3b shows the time evolution of the total area of the droplets A , where $A \equiv \frac{1}{L} \sum_{i=1}^N r_i$, where N denotes the number of the droplets, and r_i the radius of

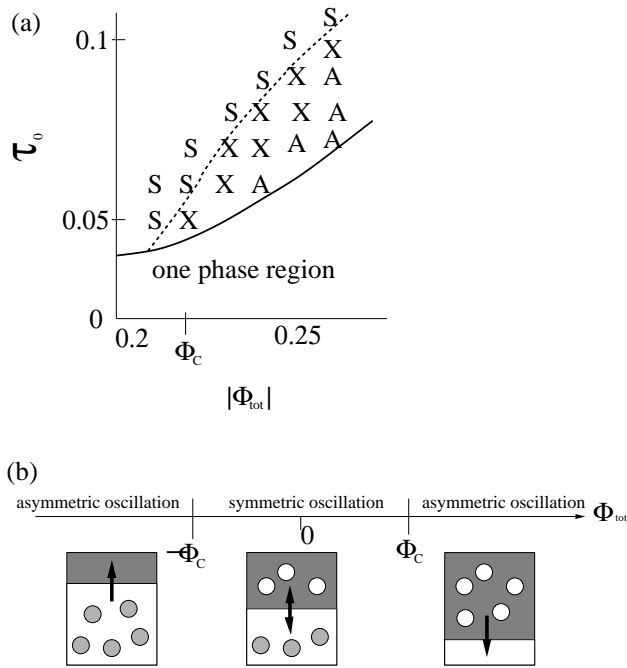


FIG. 5: (a) Phase-diagram in the $|\Phi_{tot}| - \tau_0$ plane for systems for cooling rates ξ in the range $2.8 \times 10^{-6} < \xi < 3.0 \times 10^{-6}$. The area under the solid line corresponds to the one-phase region. "A" indicates asymmetric oscillations for all ξ investigated. "S" indicates symmetric oscillations for all ξ . "X" indicates a region, where depending on ξ , either both phases or only the majority phase oscillates.

(b) Sketch of the phase separation mechanism as a function of the total composition Φ_{tot} . For $-\Phi_c < \Phi_{tot} < \Phi_c$, the turbidity of both phases oscillates. For $\Phi_c < |\Phi_{tot}|$, only the majority phase oscillates if the initial temperature τ_0 is close to the binodal line.

the i -th droplet. A is a measure of the turbidity. Around $t = 2.4 \times 10^4$ in Fig.3b, droplets are nucleated in the upper phase. When a droplet is taken from the upper phase and added to the lower phase, the volume of the lower phase V_l increases (Fig.3c, around $t = 2.4 \times 10^4$). Thus the compositions of both phases move towards the binodal line (see the horizontal lines in Fig.3a). The nucleation looks like a delta function in Fig.3b, but when we zoom into the first sequence of nucleation events, it is rather a random sequence of events (Fig.3d). After this nucleation "wave", the upper phase still keeps significant supersaturation, i.e. does not reach the binodal. This is because the droplets have reached their critical size and are removed before they diminish supersaturation completely.

After the first nucleation wave, Φ_u and Φ_l are no longer equal. The lower phase, whose composition is now closer to the spinodal line, produces its next nucleation wave near $t = 2.6 \times 10^4$ (see Fig.3b). When droplets of the lower phase sediment into the upper phase, the volume of the lower phase V_l decreases (Fig.3c close to $t = 2.6 \times 10^4$). At a cooling rate $\xi = 2.3 \times 10^{-5}$, three nucleation waves are observed for each phase, before the end temperature is reached. On these nucleation waves on average 8 droplets are exchanged for a

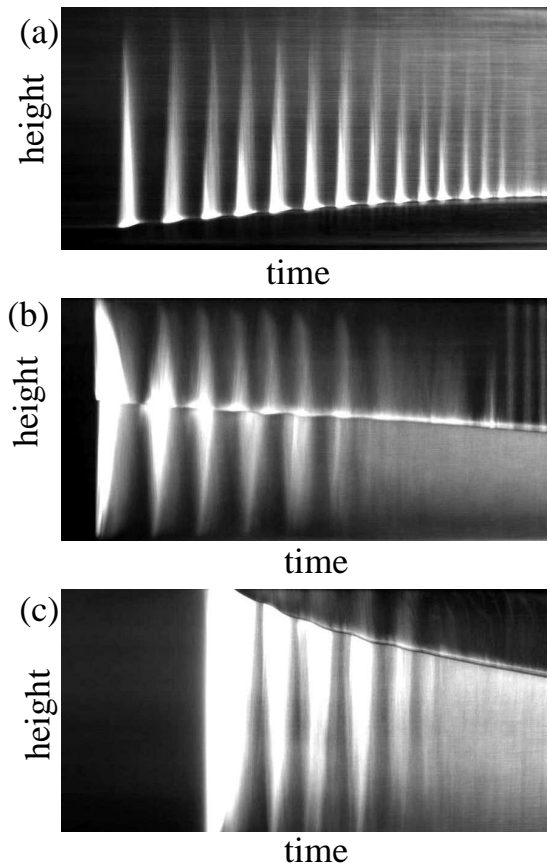


FIG. 6: Space-time plots for the composition dependence of turbidity oscillations of a binary mixture methanol/hexane. The volume fractions of methanol were C_{meth} (a)= 0.2, (b) = 0.3, (c) = 0.4. Before collecting data, the samples were prepared in the one phase region, cooled to the initial temperature ($T_c - 0.5$ K), and kept for one hour at this temperature. At the beginning, (a) and (b) are in the two-phase region, whereas (c) still remains in the one-phase region. The samples were cooled at a rate of $\xi_{exp} = 0.75 h^{-1}$ starting from ($T_c - 0.5$ K). Total time is 4000 s.

system size of $L = 32$.

In the "symmetric" case, $\Phi_{tot} = 0.0$, turbidity oscillations are observed in both phases. The volumes of the coexisting phases are changed during droplet exchange, but both volumes V_l and V_u always remain around 0.5 (see Fig.3c). In the experimentally investigated binary methanol-hexane mixture, $\Phi_{tot} = 0.0$ corresponds to an almost equal volume fraction of the lower and upper phase. This can be realized with a methanol concentration of $C_{meth} \approx 0.3$ (see Fig.1a). The experimental results (Fig.6b) qualitatively match our numerical findings. Initially the volumes of both phases are similar, and the turbidity of both phases oscillates.

For an asymmetric composition $\Phi_{tot} = 0.3$, the system exhibits a completely different scenario, Fig.4. As initial temperature we have chosen $\tau_0 = 0.1$ and for the cooling rate $\xi = 2.3 \times 10^{-5}$. With these parameters, the values of $\Phi_u(t = 0)$ and $\Phi_l(t = 0)$ are the same as for the symmetric compo-

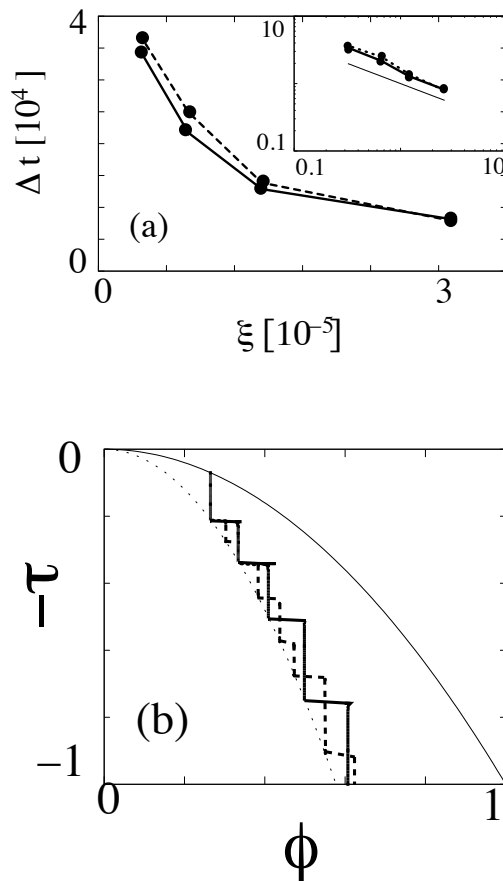


FIG. 7: (a) The period Δt of turbidity oscillations in the upper phase is plotted as a function of the cooling rate ξ for a total composition $\Phi_{tot} = 0.25$ and an initial temperature $\tau_0 = 0.07$. The solid line corresponds to a system size $L = 32$, and the dashed line to $L = 16$. In the inset, the same data are shown in a log-log plot.

(b) Evolution of the composition in the upper phase ϕ_u , for the same set of parameters as in (a), and $L = 32$. Solid line: $\xi = 6.6 \times 10^{-6}$, dashed line: $\xi = 3.2 \times 10^{-6}$.

sition, i.e. $\Phi_u(t=0) = -\Phi_l(t=0) \approx 0.32$, but the initial volumes are different, $V_u(t=0) = 1 - V_l(t=0) \sim 0.974$ or $V_u/V_l \sim 40$.

The first droplets nucleate almost simultaneously in both phases (see Fig.4b near, $t = 2.4$). However, because of the volume difference, the number of droplets which move from the upper phase, the majority phase, into the lower phase, the minority phase, is significantly larger than those moving the other way round. The composition of the minority phase approaches the binodal after the first nucleation sequence as shown in Fig.4a. The composition of the upper phase always remains close to the spinodal. As a result, we observe turbidity oscillations only in the upper phase and not in the minority phase (see Fig.4b). The sedimentation of droplets increases the volume of the minority phase V_l with each oscillation (Fig.4c).

To understand the transitions from symmetric to asymmetric oscillations better, we have plotted a "phase" diagram in

terms of the total composition Φ_{tot} and the initial temperature τ_0 , see Fig.5a. For each Φ_{tot} and τ_0 , we have investigated the cooling rates ξ between $2.8 \times 10^{-6} < \xi < 3.0 \times 10^{-5}$. In this range the turbidity of the system oscillates more than once and up to 10 times after the initial nucleation sequence. The solid line in Fig.5a corresponds to the binodal line. Starting in the two-phase region $\tau_0 > \Phi_{tot}^2$, we numerically determine the regions where asymmetric and symmetric oscillations show up. To the left of the dotted line, region "S" (symmetric oscillation) in Fig.5a, both phases nucleate droplets for all cooling rates ξ . To the right of the dotted line, the system shows asymmetric oscillations "A", i.e. the phase with the larger volume oscillates and the coexisting phase does not. In the region "X", it depends on the actual value of ξ , whether the oscillations are symmetric or asymmetric. Below the critical composition, $|\Phi_{tot}| < \Phi_c \approx 0.21$, both phases oscillate for all τ_0 and ξ .

Asymmetric oscillations are observed, when the volume difference between both phases is sufficiently large at the initial condition. In this case, the composition of the minority phase is changed by droplets expelled from the majority phase to such an extent that supersaturation remains below the threshold for nucleation. The volume ratio between the upper and the lower phase increases with increasing $|\Phi_{tot}|$. Furthermore, for an initial temperature τ_0 close to the one-phase region i.e. the binodal line in Fig.5, the volume ratio at the initial condition increases strongly due to volume and composition conservation laws. The large volume difference causes asymmetric oscillations "A". However, when we increase the initial temperature τ_0 far into the two-phase region in Fig.5a, the volumes of both phases approach each other and finally, the minority phase has a chance to nucleate droplets, too. This holds even if $|\Phi_{tot}| > \Phi_c$. For large ξ , i.e. for very fast cooling, we observe only a small number of oscillations. The system resembles the asymmetric case, although both phases oscillate for small ξ (region indicated by "X"). To compare our results with experimental data, the initial temperature τ_0 should be assigned a value close to the one-phase region. With such an initial temperature, our model predicts that both phases oscillate in the region $\Phi_{tot} < |\Phi_c|$, while for $\Phi_{tot} > |\Phi_c|$, asymmetric oscillations are observed (see Fig.5b).

To test our predictions experimentally, we have prepared different mixtures of hexane and methanol. For $C_{meth} = 0.2$ (Fig.6a), the upper phase (hexane-rich phase) has initially the larger volume. In this case, the upper phase, i.e. the majority phase, shows turbidity oscillations and the lower does not. The volume of the lower phase increases due to droplet transfer from the upper phase. This scenario corresponds to the asymmetric oscillations in the model as shown in Fig. 4. As C_{meth} increases, the initial volumes of the lower and the upper phase become equal. At $C_{meth} = 0.3$, symmetric oscillations are observed, Fig.6b. Increasing C_{meth} further the lower phase initially has the larger volume, shown in Fig.6c. In this case, the oscillations of the lower phase are more pronounced than those of the upper phase.

B. The period of the oscillation

To check the cooling rate dependence, we used $\Phi_{tot} = 0.25$ and $\tau_0 = 0.07$, i.e. a composition where the upper phase always oscillates while the lower one does not (see Fig.5a). The cooling rate ξ was changed between $3.2 \times 10^{-6} < \xi < 2.6 \times 10^{-5}$. Even faster cooling rates do not cause any oscillation, because nucleation and coarsening are too slow compared to the time the system needs to reach its end temperature τ_{end} . The finite size of the system prevents to use of even lower cooling rates, since in the latter case, one can observe only one or two droplets at any oscillation.

As the cooling rate was defined to keep the average mass transfer constant, the oscillation period of the upper phases Δt hardly varies with time if ξ is constant. The average oscillation period Δt decreases for an increasing cooling rate, Fig.7a. A log-log plot (inset of Fig.7a) indicates a power law relation between the cooling rate ξ and the oscillation period Δt , $\Delta t \sim \xi^\alpha$, where $\alpha \sim -0.6$. The experimental results for the hexane-methanol binary mixture show a similar relation $\Delta t \sim \xi^{\alpha'}$ with an exponent⁴ $\alpha' = -0.6 \pm 0.15$.

V. DISCUSSION

We investigated the CH equation with a special procedure to model gravity describing phase separation under continuous cooling. Other than gravity, further contributions might be added to the CH equation such as hydrodynamic flow and surface tension between both phases, etc. to achieve a realistic description of the experiments. The phase diagram used in our simulations is symmetric against $\phi \rightarrow -\phi$, whereas in experimental systems, the phase diagram is slightly asymmetric. In the case of the methanol - hexane system, as shown in Fig.1a, the left branch is steeper than the right one, and the position of the spinodal line is uncertain. Another important asymmetry between the upper and the lower phase is the air-

liquid interface at the top giving rise to Marangoni convection. Nevertheless, for the question, whether either asymmetric oscillation or symmetric oscillations occur, we consider the material exchange between the upper and the lower phase due to gravity to be the crucial effect.

We note that, especially in the case of the hexane - methanol binary mixture, methanol wets the hexane-air interface bringing about a wetting layer of about $40nm$ thickness.³⁰ As the height of the sample is a few *cm*, it exceeds the thickness of the wetting layer by more than 5 orders of magnitude. Therefore, we expect that the wetting layer does not influence the period of the oscillations. Indeed, we did not observe a change of the period when replacing the air by a solid interface.

VI. CONCLUSION

Motivated by experimental observations of turbidity and specific heat oscillations in binary mixtures under continuous cooling, we investigated the phase separation of binary mixtures using the CH equation with a simplified procedure to account for gravity. We numerically observed an oscillatory instability of droplet formation. Depending on the total composition, oscillations in either both or only one of the phases occur. In the latter case, the majority phase becomes the oscillating and the minority phase the 'silent' phase, both, in experiment and in our simulations. In agreement with experimental findings and analytic studies, we found a power law relation between the oscillation period and the cooling rate.

ACKNOWLEDGEMENTS

We are grateful to J. Vollmer, S. Puri, B. Dünweg, H. Tanaka, and A. S. Mikhailov for useful discussions. This research was supported by the German Science Foundation, Vo639/11-1.

¹ A. Onuki, *Phase Transition Dynamics* (Cambridge University Press, 2002).
² L. A. Utracki, *Polymer Alloys and Blends. Thermodynamics and Rheology* (Hanser, Munich, 1990).
³ D. Vollmer, R. Strey, and J. Vollmer, *J. Chem. Phys.* **107**, 3619 (1997).
⁴ G. K. Auernhammer, D. Vollmer, and J. Vollmer, *J. Chem. Phys.* **123**, 134511 (2005).
⁵ J. Vollmer, G. K. Auernhammer, and D. Vollmer, *Phys. Rev. Lett.* **98**, 139903 (2007).
⁶ J. Vollmer and D. Vollmer, *Faraday Discuss.* **112**, 51 (1999).
⁷ A. Turchanin, R. Tsekov, and W. Freyland, *J. Chem. Phys.* **120**, 11171 (2004).
⁸ R. S. Sparks, H. E. Huppert, T. Kozaguchi, and M. A. Hallwood, *Nature* **361**, 246 (1993).
⁹ J. Vollmer, D. Vollmer, and R. Strey, *J. Chem. Phys.* **107**, 3627 (1997).
¹⁰ M. E. Cates, J. Vollmer, A. Wanger, and D. Vollmer, *Phil. Trans.*

R. Soc. A: Mathematical, Physical and Engineering Sciences, **361**, 793 (2003).
¹¹ A. J. Wagner, M. E. Cates, and J. Vollmer, *Proceedings of 3IC-CHMT, Paper Number Keynote 5*.
¹² D. Vollmer, J. Vollmer, and A. Wagner, *Phys. Chem. Chem. Phys.* **4** 1380 (2002).
¹³ J. W. Cahn and J. E. Hilliard, *J. Chem. Phys.* **28**, 258 (1958).
¹⁴ J. W. Cahn and J. E. Hilliard, *J. Chem. Phys.* **31**, 688 (1959).
¹⁵ Y. Oono and S. Puri, *Phys. Rev. Lett.* **58**, 836 (1987).
¹⁶ Y. Oono and S. Puri, *Phys. Rev. A* **38**, 434 (1988).
¹⁷ S. Puri and Y. Oono, *Phys. Rev. A* **38**, 1542 (1988).
¹⁸ H.-O. Carmesin, D. W. Heermann, and K. Binder, *Z. Phys. B* **65**, 89 (1986).
¹⁹ K. Kitahara, Y. Oono, and D. Jasnow, *Mod. Phys. Lett. B* **2**, 765 (1988).
²⁰ J. S. Langer, M. Baron, and H. D. Miller, *Phys. Rev. A* **11**, 1417 (1975).
²¹ C. Yeung, T. Rogers, A. Hernandez-Machado, and D. Jasnow, *J.*

- Stat. Phys. **66**, 1071 (1992).
- ²² S. Puri, N. Parekh, and S. Dattagupta, J. Stat. Phys. **75**, 839 (1994).
- ²³ S. Puri, Physica A **224**, 101 (1996).
- ²⁴ H. Tanaka, Phys. Rev. E **51**, 1313 (1995).
- ²⁵ H. Tanaka and T. Araki, Phys. Rev. Lett. **81**, 389 (1998).
- ²⁶ M. E. Cates, V. M. Kendon, P. Bladon, and J.-C. Desplat, Faraday Discuss., **112**, 1 (1999).
- ²⁷ P. C. Hohenberg and B. I. Halperin, Rev. Mod. Phys. **49**, 435 (1977).
- ²⁸ I. M. Lifshitz and V. V. Slyozov, J. Phys. Chem. Solids **19**, 35 (1961).
- ²⁹ W. H. Press, S. A. Teukolsky, W. T. Vetterling, and B. P. Flannery, *Numerical Recipes in Fortran* (Cambridge University Press, London, 1992).
- ³⁰ D. Bonn and D. Ross, J. Rep. Prog. Phys. **64**, 1085 (2001).